

Nitrate variability along the Oregon coast: Estuarine–coastal exchange

A.C. Sigleo^{a,*}, C.W. Mordy^b, P. Stabeno^c, W.E. Frick^d

^a U.S. Environmental Protection Agency, Western Ecology Division, 2111 SE Marine Science Drive, Newport, OR 97365, USA

^b Joint Institute for the Study of the Atmosphere and Oceans, Box 354235, University of Washington, Seattle, WA 98195-4235, USA

^c NOAA, Pacific Marine Environmental Laboratory, 7600 Sand Point Way NE, Seattle, WA 98115-6349, USA

^d U.S. Environmental Protection Agency, Environmental Effects Laboratory, 960 College Station Road, Athens, GA 30605-2720, USA

Received 14 June 2004; accepted 2 February 2005

Available online 7 April 2005

Abstract

Coastal upwelling along the Eastern Pacific provides a major source of nutrients to nearby bays and estuaries during the summer months. To quantify the coastal ocean nitrogen input to Yaquina Bay, Oregon, nitrate concentrations were measured hourly from a moored sensor during summer upwelling in August 2000 outside the jetties to the estuary. Nitrate concentrations associated with coastal upwelling were generally high (up to $34 \mu\text{mol l}^{-1}$). The high-temporal resolution of the nitrate data clearly showed variations with a period of ~ 12 h. The nitrate variations were tightly coupled with temperature variations, with warmer water corresponding to lower nitrate values ($5\text{--}20 \mu\text{mol l}^{-1}$). Discretely-collected samples defined the estuarine conditions during the same period. The estuarine samples also varied from 5 to $20 \mu\text{mol l}^{-1}$ dissolved nitrate, suggesting that the lower nitrate values were associated with water ebbing from Yaquina estuary. Model calculations, used to estimate the amount of nitrate received by the estuary, indicate that the flux of nitrate into the bay averaged $12,900 \text{ kg day}^{-1}$ during upwelling. The water chemistry at the nitrate sensor was a complex product of tidal forcing, wind-induced currents and biological utilization of nutrients. A discharge model was used to examine the ebbing tide entrainment hypothesis when ocean currents were steady. Where ocean currents change rapidly in a few hours, the plume trajectories, however, will meander horizontally, fractionate or become patchy. The model analysis supports the tidal Yaquina Bay outflow premise as a cause for nitrate and water property variations near the Yaquina Bay entrance jetties. High-temporal resolution nitrate analyses indicate that near shore coastal waters were influenced by nearby estuarine outflow as well as by coastal upwelling.

© 2005 Elsevier Ltd. All rights reserved.

Keywords: nitrate; coastal upwelling; tidal plume; Yaquina Bay; NE Pacific Ocean

1. Introduction

Summer upwelling events along the Oregon coast provide pulses of nutrient-rich water that supplement nutrient-depleted waters in coastal bays and estuaries (Atlas et al., 1977; Small and Menzies, 1981). Coastal upwelling is a seasonal occurrence in response to

northerly winds that bring cold, nutrient-rich water to the surface along the Oregon coast (Barth et al., 2000; Strub and James, 2000). In spring and early summer, the upwelling zone remains close to the coastal shelf in a relatively narrow band of cold ($<10^\circ\text{C}$) upwelled water that intensifies during the summer, resulting in numerous eddies partially regulated by benthic topography (Barth et al., 2000). Atlas et al. (1977) noted that the largest temperature changes and highest nutrient concentrations were recorded within 10 km of the coast. The actual amount of a given nutrient that might enter

* Corresponding author.

E-mail address: sigleo.anne@epa.gov (A.C. Sigleo).

an estuary and supplement summertime productivity, however, has only been estimated (Atlas et al., 1977).

Established water quality goals for the next decade include the development of techniques and models to assess and predict physical, chemical and biological conditions in coastal water bodies. Robust physical and biogeochemical models of coastal ecosystems, however, require sufficient monitoring data to initialize and verify the models. Accurate assessments of nutrient levels are needed in coastal areas to evaluate nutrient impacts on coastal ecosystems. To accomplish these goals, in-field data with sufficient temporal resolution are required to determine nutrient sources and sinks, and to ultimately calculate nutrient budgets.

Oceanographic time series that acquire high density data sets were used to resolve the temporal variability of biogeochemical processes on seasonal and inter-annual time scales (Karl and Lukas, 1996; Dickey et al., 1998; Steinberg et al., 2001). Densely populated time series data sets can capture transient events and resolve short-term temporal processes (Hydes et al., 2000; Weston et al., 2004). For example, a moored nitrate sensor used in the Bermuda Testbed program measured short nitrate pulses that preceded increased chlorophyll *a* concentrations by 12–24 h (Dickey et al., 1998). In the North Sea, Weston et al. (2004) determined the importance of the offshore plume region in processing nitrogen using a nitrate time series. Since processes such as tidal exchange, wind driven upwelling, and river runoff can cause large and rapid spikes in coastal and estuarine nutrient concentrations, high-temporal resolution data are imperative for capturing phenomena that might otherwise lead to substantial over- or under-estimations of nutrient loading.

The objective of the work reported here was to quantify the summertime coastal nitrate entering Yaquina Bay, Oregon, as a component of the annual nutrient budget for the estuary. Coastal inputs were then compared to estuarine outflows to estimate net nitrate transport. To quantify the magnitude of upwelled nitrate entering Yaquina estuary, a nitrate sensor was deployed adjacent to the estuary entrance buoy in a direct line with the entrance jetties (Fig. 1). The nitrate time series was then used to model the coastal nitrate input into the estuary for August 2000. A primary objective of the study was to determine the relative importance of the coastal ocean relative to the watershed as sources of nitrate for the bay during the upwelling season. The data were analyzed by current speed and water discharge models to interpret the observed events.

2. Study area

Yaquina Bay is a tidal estuary on the west coast of the United States (44.6°N, 124.0°W) that flows into the Pacific Ocean at Newport, Oregon (Fig. 1). Yaquina Bay has a semi-diurnal tidal regime with diurnal inequalities.

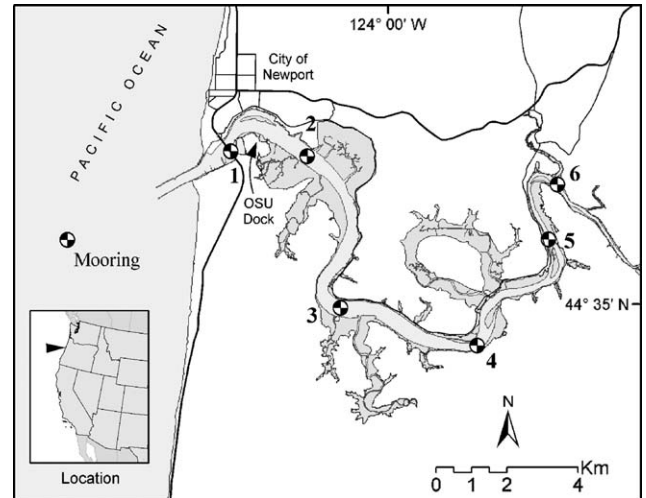


Fig. 1. The location of the mooring near the seaward whistle buoy of Yaquina Bay channel. Station 1 is located under the Yaquina bridge and Stations 2–6 are located in the main channel of the estuary.

The tide heights are 2.55 m at a mean higher high water (MHHW) and 2.34 m at mean high water (MHW) with a mean tidal range of 2.4 m (Larned, 2003; Kentula and DeWitt, 2003). Within the bay the combined marine and mesohaline zones cover 18 km² of which 40% is subtidal channel and 60% is inter-tidal mudflat, sandflat and seagrass habitat covered by *Zostera marina* and *Zostera japonica* (Larned, 2003). Both *Zostera* sp. and benthic diatoms form dense patches in the inter-tidal zones which are net sinks for NO₃, particularly during the summer months (Larned, 2003; Kentula and DeWitt, 2003; Sin, unpublished data).

The primary land use in the Yaquina watershed is silviculture. Forests are dominated by coniferous trees, although disturbed sites are frequently occupied by pioneer broad-leaved trees. Broad-leaved trees, predominantly red alder, also occur in riparian areas along streams. Nitrate in the Yaquina watershed, along with many other Oregon coastal rivers, originates from the fixation of atmospheric nitrogen by red alder (*Alnus* spp.) which forms a symbiotic relationship with the actinomycete *Frankia* spp. (Compton et al., 2003).

The region is characterized by a maritime climate with mild wet winters and cool drier summers. Yaquina River flow ranges from 0.28 m³ s⁻¹ during late summer low flow conditions to 78 m³ s⁻¹ during winter storms (Sigleo and Frick, 2003).

3. Methods

3.1. Measurements and moorings

The subsurface mooring was deployed 2.9 km from the end of the jetties outside the mouth of Yaquina Bay, Oregon, August 1–29, 2000 in approximately 30.5 m of

water near the seaward whistle buoy of Yaquina Bay entrance channel (Fig. 1). The mooring consisted of a WS EnviroTech NAS-2E nitrate sensor at 15 m, a Sea-Bird Electronics, Inc SeaCat temperature and salinity sensor at 18 m and an Aanderaa Enterprises RCM-9 current meter with a temperature sensor at 20 m depth. The recorder on the RCM-9 malfunctioned, resulting in data being recorded for 2 days, followed by a 2-day gap. This pattern persisted throughout the deployment. The RCM-9 sampled every 15 min, and the NAS-2E and SeaCat sampled hourly.

In the coastal zone outside the bay, separate nutrient and chlorophyll *a* samples were collected just below the water surface during mooring deployment and recovery, and from the adjacent surf zone north of the north jetty weekly during the month. Discrete nitrate samples were compared to nitrate values collected from the NAS-2E. All discrete samples were collected at high tide. The Yaquina Bay jetties blocked direct transport of bay water to the surf zone such that the samples were representative of coastal waters (Takesue and van Geen, 2002).

Within Yaquina Bay nutrient samples were collected at the Oregon State University (OSU) dock at high tide weekly to determine the nitrate concentration entering into the estuary. Water samples (0.5 m depth) also were collected with Niskin bottles along the main channel of the Yaquina River at high slack tide June 28, July 26 and August 24, 2000 to measure river channel temperature, conductivity and dissolved nitrate concentrations.

The NAS-2E was programmed to collect and analyze water samples for dissolved nitrate + nitrite hourly (Hydes et al., 2000). Because nitrite in discrete samples comprised less than 1% of the nitrogen species at this site, it is not discussed further, and nitrate + nitrite will be treated as nitrate. The sensor was automatically calibrated every 6 h using an onboard standard (OBS). Blanks were determined from measurements of the standard or sample absorbance without reagents prior to the measurement of each sample or standard. The NAS samples were prefiltered with an aquarium aerating filter over the inlet tube. Standard and sample analytical methods were identical and consisted of the reduction of nitrate to nitrite in a cadmium column, and the formation of a red azo dye by nitrite complexation with sulfanilamide and *N*-1-naphthylethylenediamine. The complexed nitrite was measured colorimetrically to determine concentrations of nitrate.

The OBS was prepared according to guidelines provided by the Joint Global Ocean Fluxes Study (JGOFS) offices (Gordon et al., 1993), including calibration and temperature correction of glassware and pipettes, stepwise dilution of primary and secondary standards in distilled-deionized water, and preparation of working standards in low-nutrient seawater with a known nitrate concentration. Three batches of primary, secondary, and working standards were prepared with

a final concentration of 15 $\mu\text{mol l}^{-1}$ nitrate. The standards were pasteurized at 60 °C for 6 h. (Aminot and K erouel (1998) suggested pasteurization at 80 °C, but at the higher temperatures the storage containers failed.) After pasteurization, nitrate concentrations in the standards agreed within 0.1 $\mu\text{mol l}^{-1}$ of the expected nitrate concentration. One of the standards was deployed as the OBS, and the other two standards were refrigerated. To verify OBS stability, the OBS was analyzed before and after deployment along with the standards prepared in parallel and stored refrigerated. The OBS and the parallel standard concentrations were 15.3 $\mu\text{mol l}^{-1}$ and 15.1 $\mu\text{mol l}^{-1}$, respectively.

Discrete water samples for nitrate and chlorophyll *a* were filtered on pre-combusted Whatman GF/F filters that were submerged immediately in 90% acetone. Chlorophyll *a* filters were extracted overnight at -4 °C in the dark, and analyzed at EPA using a Turner Designs Model 10 fluorometer. The filtrate for nutrient analyses was frozen and shipped to a contract laboratory for analysis of nitrate within 30 days using a Lachat autoanalyzer (MSI Analytical Laboratory, UC Santa Barbara, CA). Replicate nitrate samples collected during the mooring deployment and recovery were transported on ice to the Pacific Marine Environmental Laboratory (PMEL), and frozen until analyzed several days later using an autoanalyzer composed of components from Perstorp and Alpkem.

Tide data were obtained from the Newport station at the OSU dock at South Beach, OR (NOAA Station 9435380). Hourly wind data were available from the National Data Center for Station NWP03 on the Newport South Jetty at South Beach.

3.2. Nitrate flux calculations

Net nitrate fluxes into and out of the estuary were estimated using Eq. (1),

$$F = \sum_{i=t_1}^{t_2} [\text{NO}_3]_i v_i A_i \quad (1)$$

where F was the net integrated nitrate flux, or flux summation, through the mouth of the jetties from hour t_1 to hour t_2 , and, $[\text{NO}_3]_i$ ($\mu\text{mol l}^{-1}$) and v_i were the average nitrate concentration and velocity (speed) through the cross-sectional area between the jetties, A_i , during hour i . The sign of the velocity determined gain or loss of nitrate.

It was assumed that during flood tide nitrate concentrations at the mouth of the jetties were equal to a constant concentration value in upwelled water, nominally 30 $\mu\text{mol l}^{-1}$. During ebb tide, the August 2000 Yaquina Bay transect values were used to estimate concentrations in the water between the jetties. This concentration was a function of distance traveled by a water parcel in moving towards the mouth from its

“source” region, in other words, from its estimated maximum upstream penetration into the estuary. In 1-km increments, it was assumed that the nitrate level between the mouth of the estuary and at 1 km into the bay was $30 \mu\text{mol l}^{-1}$ near high slack water (the first kilometer of travel of a parcel), decreased linearly, presumably due to biological uptake, to $20 \mu\text{mol l}^{-1}$ at 3 km, and decreased further to the minimum level of about $5 \mu\text{mol l}^{-1}$ between 3 km and 12 km up-estuary. Both velocity and cross-sectional area were functions of tide height. The cross-sectional area was estimated using Eq. (2):

$$A_i = 2135 + 300(h_i - h_{\text{MLLW}}) \quad (2)$$

where the approximate cross-sectional area at the reference elevation (MLLW) was 2135 m^2 , the approximate distance between the jetties was 300 m, h_i was the tide elevation at hour i , and h_{MLLW} was the reference elevation. Area estimates were based on soundings and dimensions shown on NOAA Nautical Chart 18581 (NOAA, 1984).

3.3. Velocity estimates between the jetties: the Yaquina Bridge Current Speed Model (YBM)

Velocity estimates at the mouth of the bay, required in Eq. (1), were obtained using an empirical current speed model (Chapman et al., 1997). The model was verified with data obtained from the test deployment of a 600 kHz Acoustic Doppler Current Profiler (ADCP) deployed for a week in September 1995 under the Yaquina Bay Bridge (Station 1) near the southern edge of the shipping channel (Fig. 1).

The basic equation used in YBM to estimate current speed at Yaquina Bridge is

$$v_i = \frac{(dV/dt)_i}{A_i} \quad (3)$$

where $(dV/dt)_i$ is the time rate of change of the volume in the bay upstream of the estuary cross-section at the bridge, A_i . The estimate represents average conditions over time period i . The upstream volumes were based on estimates of the product of the upstream estuary area at discrete tide levels spaced on 10 cm vertical increments and the change in tide height over time period i .

YBM allows both observed and predicted estimates of tide height, the latter giving it a prognostic capability. Harmonic tide models in which the governing astronomical frequencies are known and the tidal amplitudes and phases at particular sites are determined empirically can accurately estimate tide heights under average atmospheric conditions. YBM adapts Wallner's tide model (1995) for this purpose, although for this work, observed tide heights from the NOAA station were used in the final calculations.

3.4. Estuary–coastal interactions: the Prych-Davis-Shirazi (Windows-based) plume model (PDSW)

To understand nitrate concentrations and other data observed offshore in relationship to events in the estuary it was necessary to establish whether observed variations were due to oceanic effects, such as internal tides causing variations at a fixed depth due to the vertical movement of a stratified water column, or, the estuarine plume impinging on the instruments, or both. It must be borne in mind that, although the freshwater flow was negligible, the estuary tidal prism discharges approximately $27 \times 10^6 \text{ m}^3$ of water on ebb tide, at about $2000 \text{ m}^3 \text{ s}^{-1}$, that will produce a large jet of water discharging between the jetties twice each day.

However, this point is moot if the water body does not reach the instrument mooring prior to the dissipation of its properties by dilution or due to its deflection out of the path to the instruments by alongshore currents. The Prych-Davis-Shirazi Windows (PDSW) surface discharge plume model (Davis, 1999) was used to provide estimates of dilution and deflection (Frick et al., 2003). PDSW uses an entrainment hypothesis to complete the water body, or plume, conservation of mass equation. Entrainment is the dilution process by which the plume incorporates ambient fluid. An increase in ambient current speed typically leads to more rapid dilution. In addition, it uses a reflection technique to simulate the buoyant spreading of the plume at the free surface. PDSW is a steady-state model and sequential runs are necessary to infer changes in plume variables with time, making interpretation more difficult. In fact, hodographs for the site would imply that the plume typically meandered as its parcels flowed oceanward during ebb tides, accelerating and decelerating while mixing with ocean water of varying dynamic properties. In addition to dilution, PDSW also predicted in-plume velocity isopleths, plume depth in the water column, and plume deflection.

4. Results

4.1. Measurements

Several short periods of upwelling-favorable (northwest to north) winds and downwelling-favorable winds were evident in the time series (Fig. 2A). Two of the strongest upwelling-favorable wind events were observed at the beginning (August 1–4, $5\text{--}14 \text{ m s}^{-1}$) and near the end (August 20–24, $5\text{--}11 \text{ m s}^{-1}$) of the month. Associated with northerly winds were higher salinities (> 33.8 , Fig. 2B), and lower temperatures (down to $7.8 \text{ }^\circ\text{C}$, Fig. 2C). Moderate northerly winds were observed from

August 6–17 ($\sim 1.5\text{--}6\text{ m s}^{-1}$) along with a period of slight warming and freshening, presumably due to the erosion of the strong upwelling front. Strong upwelling-favorable winds were also observed from August 21–23 ($4\text{--}9\text{ m s}^{-1}$). Warmer temperatures on August 18–19 and 24 were associated with southerly winds.

Nitrate in the time series varied from 5 to $34\text{ }\mu\text{mol l}^{-1}$ with a semi-diurnal frequency (Fig. 2D). Maximum nitrate concentrations at the beginning of the month, about $32\text{ }\mu\text{mol l}^{-1}$, gradually decreased to $27\text{ }\mu\text{mol l}^{-1}$ during the first 14 days, suggesting steady biological utilization combined with reduced upwelling (Fig. 2D). The monotonic decline was followed by several days of extreme variability, then the maximum again increased to about $31\text{ }\mu\text{mol l}^{-1}$. Despite semi-diurnal oscillations, the maximum daily nitrate concentrations indicate sustained upwelling for the month of August. The temporal resolution of the NAS nitrate data showed changes with a period of $\sim 12\text{ h}$ (Fig. 2D). Nitrate variability was tightly coupled to temperature changes (Fig. 2C), with warmer water corresponding to lower nitrate.

Nitrate concentrations from the moored NAS were compared with nitrate concentrations in samples collected at high tide from the nearby surf zone and at the OSU dock (Fig. 2D). The NAS and surf zone nitrate concentrations were found to be in excellent agreement, and differed by $<0.1\text{ }\mu\text{mol l}^{-1}$. Nitrate concentrations at the OSU dock, however, were generally 30% lower than those of the NAS/surf zone concentrations. Samples collected when the NAS was deployed had relatively low nitrate ($18 \pm 1.0\text{ }\mu\text{mol l}^{-1}$, $n = 2$), possibly due to a foregoing downwelling event.

Nitrate within the Yaquina estuary ranged from $31\text{ }\mu\text{mol l}^{-1}$ at the ocean side, decreased to less than $5\text{ }\mu\text{mol l}^{-1}$ at stations 4 and 5, and increased to approximately $20\text{ }\mu\text{mol l}^{-1}$ in the freshwater part of the system (Fig. 3).

Nitrate and temperature showed a significant inverse relationship ($r^2 = 0.71$, $n > 700$). Prior to August 19, 12-h oscillations of nitrate were typically $2\text{--}5\text{ }\mu\text{mol l}^{-1}$. However, from August 19–27, nitrate concentrations varied as much as $10\text{ }\mu\text{mol l}^{-1}$ every 12 h. The greatest variations were on August 19 when temperatures were $>10\text{ }^\circ\text{C}$ and nitrate concentrations ranged from 4.2 to $30\text{ }\mu\text{mol l}^{-1}$. These oscillations coincided with a full moon on August 19.

Chlorophyll *a* concentrations from the Oregon coast ranged from 1.4 to $6.6\text{ }\mu\text{g l}^{-1}$ and in Yaquina Bay (OSU dock) the range was from 0.9 to $3.5\text{ }\mu\text{g l}^{-1}$ (Fig. 4). Both ranges are characteristic of active summertime primary productivity (Small and Menzies, 1981).

4.2. Current velocity estimates between the jetties

The prognostic YBM model velocity predictions and ADCP measurements are compared in Fig. 5. Predicted

velocities at the bridge were assumed to be representative of along-channel velocities at the mouth of the estuary between the jetties. In fact, they would be somewhat larger at the end of the jetties ($<10\%$) due to the volume of water between the bridge and the end of the jetties that would add to the total flow as the tide height changes. Thus, the estuary plume considered subsequently was not based on the maximum possible discharge strength.

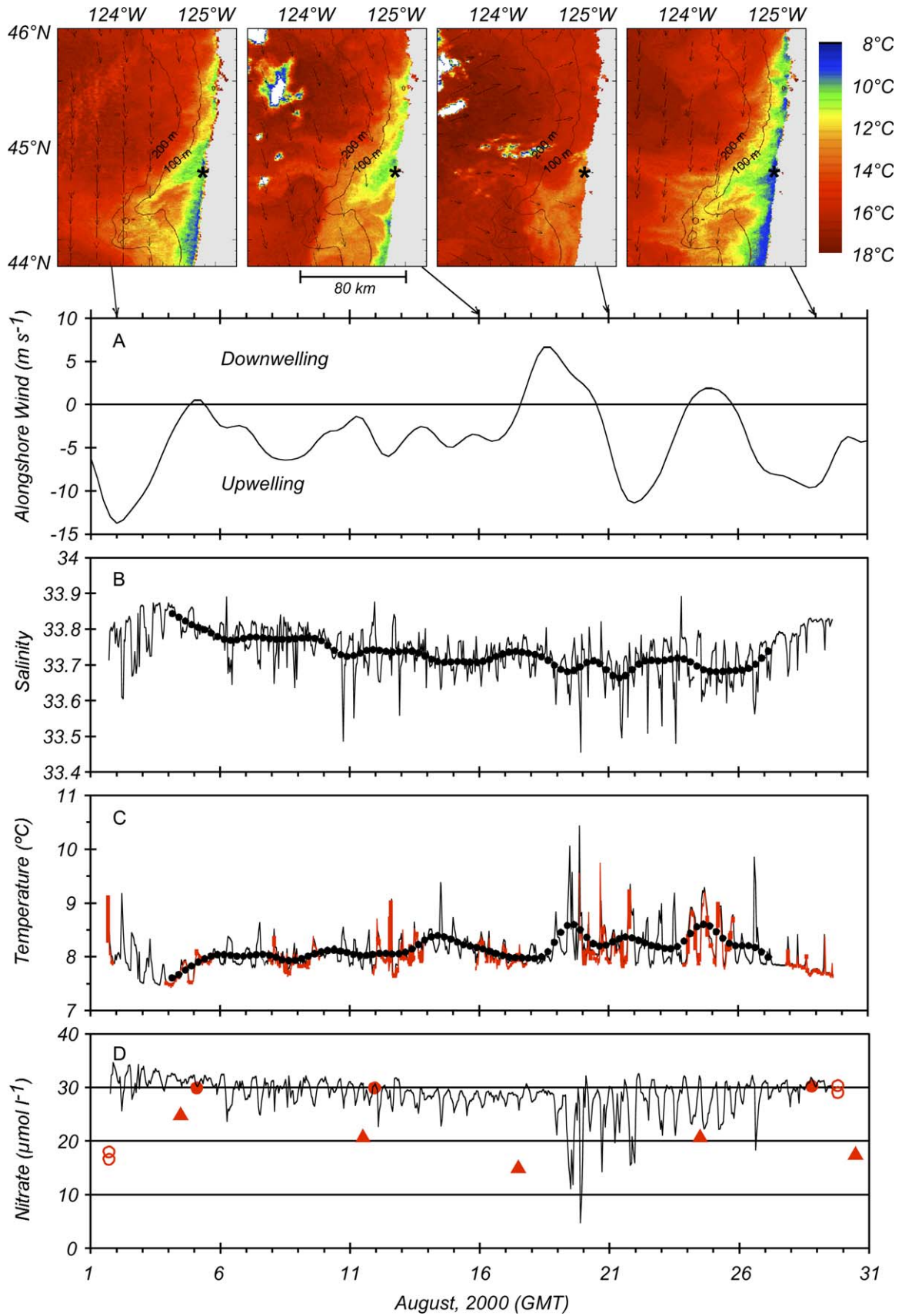
Current speeds predicted by the YBM model compared favorably with measured data (Fig. 5). The maximum ebb flow at the bridge for August 2000 was $2140\text{ m}^3\text{ s}^{-1}$ (Table 1).

4.3. Nitrate fluxes

The EPA Visual Plumes discharge model was used in combination with nitrate concentration data and velocity measurements to estimate the dilution and trajectory of the ebbing Yaquina Bay water mass as it flowed toward the mooring. With a discharge velocity of 0.81 m s^{-1} , a distance of 225 m between the jetties, a channel depth of 13.2 m, and an alongshore current of 0.01 m s^{-1} , the PDSW surface discharge model (Davis, 1999) predicts that the plume will contact the instrument at 0.5 m s^{-1} (Fig. 6). In traversing the interval between the jetties and the instruments, it increased to a width of about 2600 m and its centerline axis was deflected only about 100 m off a straight trajectory. Based on a representative upwelling coastal water temperature of $8\text{ }^\circ\text{C}$ and an assumed plume temperature of $9\text{ }^\circ\text{C}$, representing some warming in the estuary, the predicted plume depth was over 20 m, sufficiently deep to contact all three moored instruments. The travel time was $>2\text{ h}$, so that the arrival of the plume lagged behind the onset of ebb flow.

Example PDSW predictions for the Yaquina estuary plume corresponding roughly to maximum discharge conditions on an average ebb tide (0.81 m s^{-1}) are given in Fig. 6 for two alongshore current speeds, 0.01 and 0.1 m s^{-1} . Surface isopleths are shown but the plume depth, assuming a $1\text{ }^\circ\text{C}$ temperature elevation in the plume, penetrated to the depth of the moored instruments. The predictions show that persistent currents in excess of 0.1 m s^{-1} would prevent a plume signal from being observed at the mooring. Greater deflecting currents followed by weaker, reversing along shore currents, could move parcels back into the path of the instruments.

The model calculations indicate that the total flux of nitrate into the bay for August 2000 was 546,000 kg, the outflow was 152,000 kg and the net nitrate gain was 394,000 kg, or 394 tonnes. The net nitrate flux, or nitrate gain to the estuary averaged $12,900\text{ kg day}^{-1}$ (Table 1).



5. Discussion

Summer water properties along the Oregon coast are determined largely by coastal upwelling driven by northerly winds (Hickey and Banas, 2003). In August 2000, satellite images of sea-surface temperatures (SST) overlain by NCEP wind vectors provided a summary of meteorological and oceanographic conditions over the shelf during the NAS deployment (Fig. 2). The consistently high maximum nitrate concentrations indicated that sustained upwelling persisted throughout the month, despite minor downwelling episodes. Low temperatures (8 °C) and high nitrate concentrations ($> 30 \mu\text{mol l}^{-1}$) observed in August 2000 were similar to previously reported characteristics of upwelled water along the Oregon coast (Atlas et al., 1977; Small and Menzies, 1981; Barth et al., 2000).

The high-temporal resolution of the nitrate data clearly showed fluctuations with a period of ~ 12 h (Fig. 2D). Surveys along the Oregon coast indicate significant patchiness and horizontal gradients in temperature, salinity and nutrients (van Geen et al., 2000) that, in combination with strong meridional flow, might result in the tidal scale spikes observed in the time series. The currents were dominated by tides with a net flow of 1.5 cm s^{-1} along a bearing of 335° true and a tidal amplitude of 25 cm s^{-1} , although the mean flow was wind driven. Variations in water properties occurred when different water masses flowed over the moored sensors. To understand nitrate variations and to evaluate the nature of the different water masses, it was necessary to establish whether the observed variations were from internal tides causing variations at a fixed depth due to the vertical movement of a stratified water column, oceanic processes such as upwelling/relaxation, or to the estuarine discharge plume impinging on the instruments.

5.1. Vertical stratification

Internal tides might produce changes similar to tidal estuarine discharge plumes if ocean properties were depth stratified such that properties measured at fixed heights above the bottom change as the density surfaces move up and down with the internal tide. The effects of internal tides and upwelling/relaxation nutriclines would be indicated by density stratification at the mooring. Temperature stratification was examined by superimposing the Sea Cat and RCM-9 temperature data at 18 and 20 m, respectively (Fig. 7). The two temperatures were

nested indicating that there was no stratification between them, nor was there a systematic time lag between the two data sets as would occur if they were from different stratified water masses. In other words, the temperatures at these depths did not show a phase shift that would be expected if a density discontinuity reached the upper instrument before affecting the lower one some time later. The temperature results do not support the theory that nutriclines or internal tides are primary features in this relatively shallow water environment.

High nitrate concentrations in the discrete samples from the surf zone also suggest an absence of stratification since water in the surf zone of southern Oregon was reported to originate from 100 to 150 m depth at 45 km offshore, and was transported onshore in the shelf bottom layer during upwelling (Takesue and van Geen, 2002). Specifically, Takesue and van Geen (2002) demonstrated that nitrate-enriched coastal upwelling source waters reached the surf zone. Thus, our surf zone samples should represent recently upwelled water, as the nitrate concentrations suggest (Fig. 2D). Salinities observed in the moored data set were consistent with offshore water moving along the shelf bottom layer and upwelling at the coast (van Geen and Husby, 1996). Waves and internal waves may also affect the water mass, but appear to be minor in importance with respect to understanding nitrate variations at the mooring.

5.2. Estuarine–coastal exchange

The largest ranges in temperature, salinity and nitrate coincided with maximum tidal excursions associated with the spring tide on August 19. The highest temperatures and lowest nitrate concentrations during the following ebb tide suggest that the extreme values observed at the mooring were produced by a greater fraction of Yaquina Bay estuarine water. River runoff is negligible in summer (average $0.7 \pm 0.1 \text{ m}^3 \text{ s}^{-1}$) and the input of river nitrate to central Yaquina Bay is minor (Sigleo and Frick, 2003). From Fig. 5, it is apparent that the Yaquina estuary between Stations 3 and 5 was a net sink for coastal nitrate during the summer rather than a source of nitrate to the coastal ocean. The temporal resolution of the NAS nitrate data showed changes with a period of ~ 12 h (Fig. 2D). The changes appear to be tightly coupled to temperature changes, with warmer water corresponding to lower nitrate, suggesting nitrate uptake within the water column or in shallower warmer

Fig. 2. AVHRR satellite images of sea-surface temperature overlain by NCEP wind vectors (top panel). The panels correspond to (A) alongshore wind speed, (B) salinity, (C) temperature, and (D) nitrate. The nitrate time series includes discrete sample data from the surf zone (filled circles), the mooring site during deployment and recovery (open circles), and from the OSU dock (triangles). The temperature time series includes data from the Sea Cat (black) and intermittent data from the RCM-9 (red). A 6-h filter was applied to winds, temperature and salinity, and both filtered (open circles) and unfiltered results are presented for temperature and salinity.

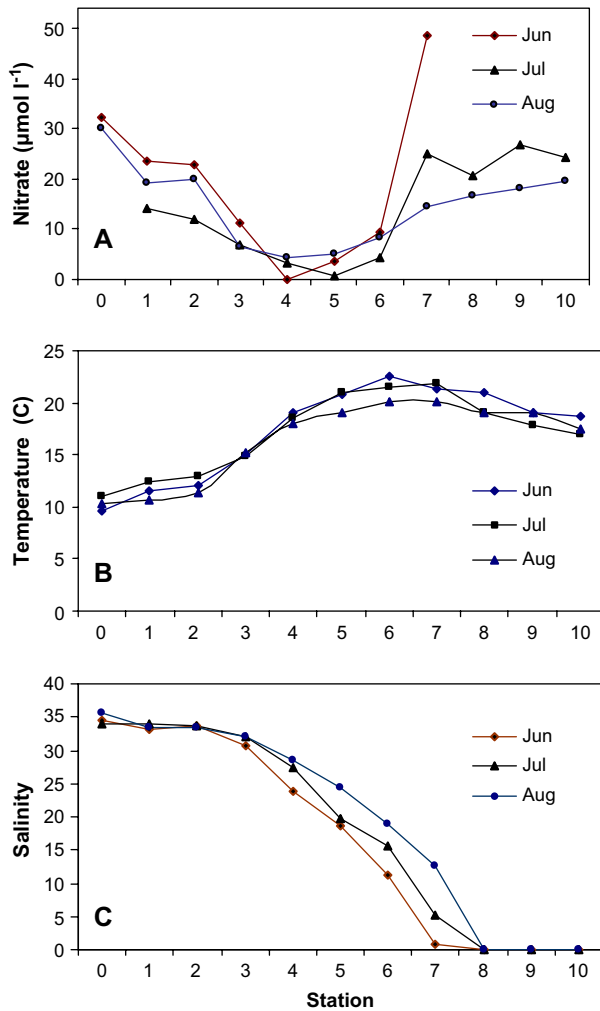


Fig. 3. Dissolved nitrate concentrations, temperature and salinity along the main channel of the Yaquina River and estuary at high slack tide to maximize the coastal component for June, July and August 2000. The estuary station locations are shown in Fig. 1.

environments such as the vegetated inter-tidal regions of the estuary (Kentula and DeWitt, 2003; Larned, 2003).

Although the freshwater river flow was negligible at the time of this study ($< 1 \text{ m}^3 \text{ s}^{-1}$), the estuary discharge on ebb tide consisted of a large water mass that produced a focused discharge of up to $2000 \text{ m}^3 \text{ s}^{-1}$ between the jetties twice every day. The jetties, in fact, function as a nozzle. As the Columbia River has a discharge plume noticeable in high altitude photographs (Hickey and Banas, 2003) the Yaquina estuary also exhibits a modest discharge plume along the coast due to the discharge of its substantial tidal prism. Hickey and Banas (2003) note that other than the Columbia plume, river plumes along the coast are relatively small, and that their traceable effects in satellite imagery are limited to one or two tidal excursions.

If nitrate were depleted within the estuary, ebbing tidal flow would discharge lower nitrate water to the near shore coastal ocean in expanding plumes (Fig. 6).

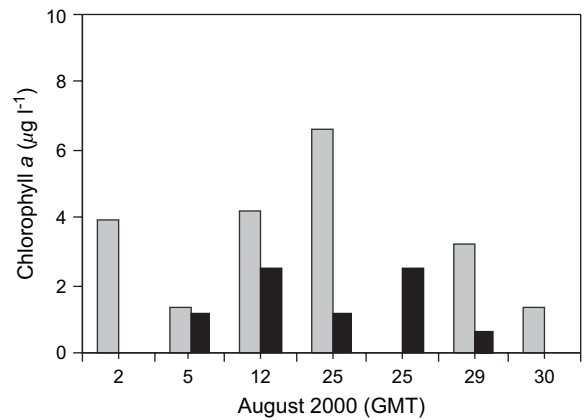


Fig. 4. Chlorophyll *a* concentrations from the surf zone (grey) and OSU dock (black).

Large negative (offshore) currents are frequently associated with ebb tides and the speeds, sometimes in excess of 0.2 m s^{-1} , agree with the predictions of the plume model (Fig. 6). Thus the large offshore velocities measured at the buoy can largely be attributed to the estuarine plume. High offshore velocity, lower nitrate, lower salinity, and warmer temperatures reflect the passage of the un-deflected plumes. Intermittent plume parcels with smaller offshore velocities travel more circuitous paths as the alongshore component of the current changes direction and causes the plume trajectory to meander (Fig. 8). When the plume was deflected, the offshore velocity component was small and water properties at the mooring were more typically coastal in character, as observed for August 20, whereas the un-deflected plume was responsible for lower nitrate concentrations that originated from the estuarine nitrate-depleted water, as on August 24–25 (Fig. 8).

The steady-state model utilized in this paper was a cross-sectionally integrated average of the actual ebbing plume, a transient phenomenon, pulsing and undulating in response to both changes in Yaquina estuary effluent velocity and changing ambient ocean currents. As the plume efflux velocity increases after slack tide, the total lag time is expected to be longer than 2.5 h. Efforts to statistically analyze the significance of relationships between variables were confounded by variable lag times. Variable lag times are expected in the plume hypothesis. Depending on the deflecting current strength and the amount of plume entrainment, the plume travel time between the end of the jetties and the instruments will vary substantially. Highly diluted and (or) deflected plumes that graze the instruments, resulting in smaller temperature rises and current changes, will take longer to traverse the distance between the jetties and the instrument mooring. Conversely, concentrated, high temperature plume parcels will reach the instruments in the least time. Thus the lag time between tide and plume signal will be variable. This variability is now

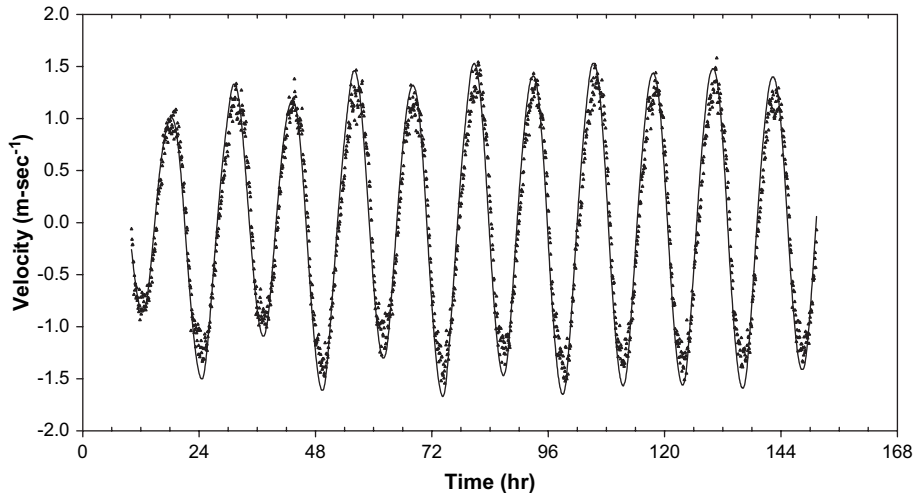


Fig. 5. Yaquina Bridge simulated current model (solid line) and observed ADCP data (dots) for September 5–11, 1995.

estimated based on the temperature rising at the instrument in relationship to the timing of the ebb cycle. Referenced to the end of the ebb cycle (the time that the estuarine plume ceases), this lag averages only a few minutes, however, the standard deviation is approximately 3 h. Thus about two-thirds of the plumes judged to reach the mooring under favorable conditions (i.e., those not deflected by strong alongshore currents) reach the mooring between mid-ebb tide to about 3 h after cessation of plume formation (end of ebb tide).

Despite the time lag, the model predictions appear to represent the effects of the plume on water properties at the buoy. If alongshore currents are weak, on the order of 0.01 m s^{-1} , the YB plume will pass over the mooring with a centerline velocity of 0.5 m s^{-1} . Southward ambient flow of 0.01 m s^{-1} is within the reported range during summer upwelling (Hickey and Banas, 2003). An alongshore current of at least 0.10 m s^{-1} is required to deflect the plume out of the path of the buoy (Fig. 6). Within this range of alongshore currents, 0.10 m s^{-1} southerly to 0.10 m s^{-1} northerly currents, the average dilution at a trajectory distance equal to the distance to the buoy is about 5:1 and the centerline dilution is about 2.5:1. The centerline dilution determines the maximum excursions of properties in parcels of fluid originating in the bay and impacting the instrument. The predicted

dilutions imply, for example, that a $20 \mu\text{mol l}^{-1}$ nitrate deficit in Yaquina Bay effluent concentration leaving the jetties, after mixing with ocean water, would give a $22 \mu\text{mol l}^{-1}$ nitrate concentration at the instrument

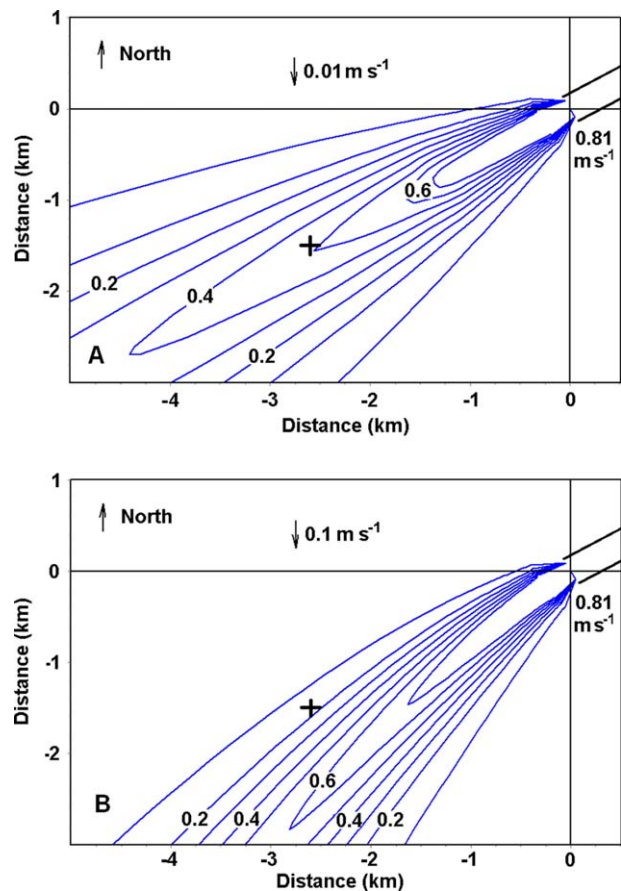


Fig. 6. Predicted spatial distribution of Yaquina estuary ebb flow plume for the ambient current conditions of (A) 0.01 m s^{-1} and (B) 0.1 m s^{-1} . Isotachs units are m s^{-1} . The plus (+) symbol indicates the mooring location. After Frick et al., 2004.

Table 1
Nitrate fluxes entering and exiting Yaquina Bay entrance channel, August 2000

Property	August 1–30
Integration period (h)	730
Nitrate flux in (kg)	546,000
Nitrate flux out (kg)	152,000
Net August nitrate gain (kg)	394,000
Average daily N gain (kg)	12,900
Max water flow ($\text{m}^3 \text{ s}^{-1}$)	2250

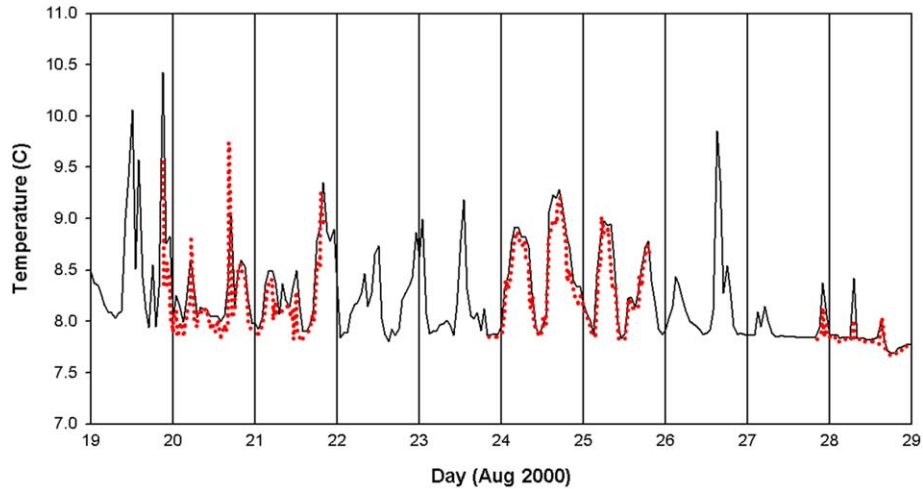


Fig. 7. Comparison of temperature data from the Sea Cat at 18 m depth (black) and the RCM-9 at 20 m depth (red dotted line).

mooring. Such nitrate values were in fact observed at the mooring during ebb flow from Yaquina Bay (Fig. 2D). Large negative (offshore) velocities were also frequently recorded, although their existence was not always clearly caused by the plume (Fig. 8). It is important to note that the model results represent the average of temporally and spatially heterogeneous plume variables (Mantovanelli et al., 2004).

The plume model and the data record at the mooring strongly support the hypotheses that Yaquina Bay estuarine water frequently flowed past the mooring and that the corresponding low-nitrate values indicated the presence of low-nitrate Yaquina Bay water. Because water entering the bay was generally coastal seawater, we conclude that the coastal ocean was a source of nutrients for Yaquina Bay as previously reported

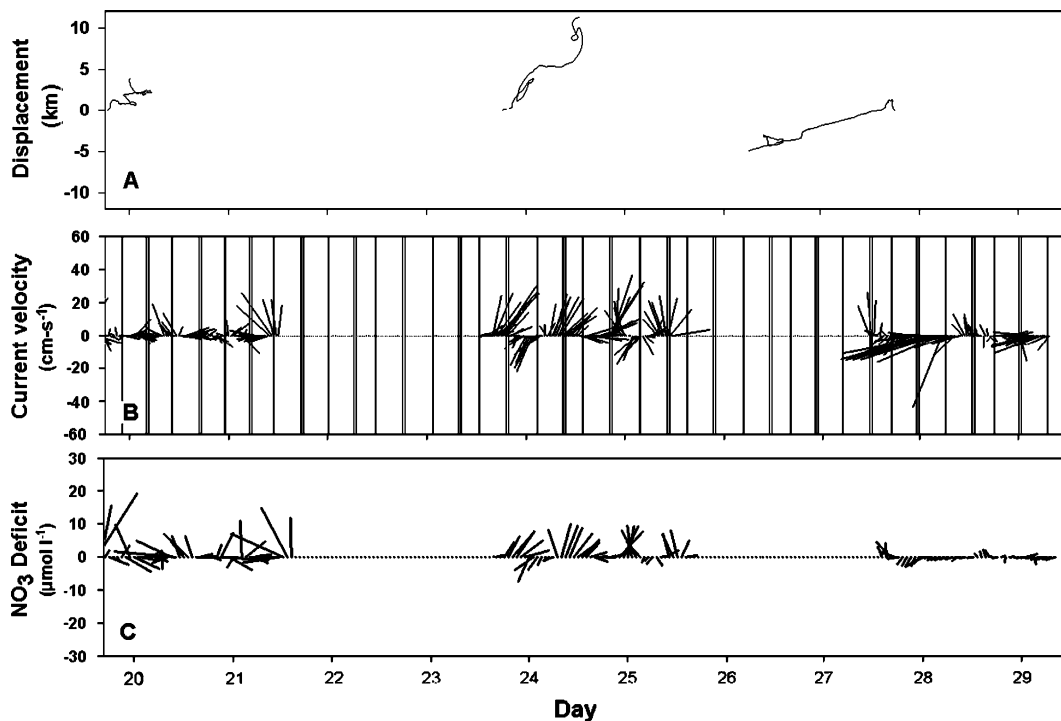


Fig. 8. Estimated horizontal water parcel movement based on integration of the RCM-9 velocities (top), RCM-9 current velocities (middle), and difference in estimated oceanic ($30 \mu\text{mol l}^{-1}$) and observed NAS nitrate concentrations (bottom, $\mu\text{mol l}^{-1}$), for 20–29 August 2000. West is toward the top and North is to the right. The RCM-9 measured every 15 min and the NAS made measurements hourly with every sixth hour missing due to the onboard standard. The beginning of ebb tide is represented by double vertical lines in the middle panel, and the beginning of flood tide by single vertical lines.

(Atlas et al., 1977). Thus, the observed semi-diurnal variability resulted from oscillation between upwelled ocean water and outflow from Yaquina Bay.

5.3. Nitrate flux

The net flux of nitrate entering the bay on typical spring and neap tide cycles was estimated using the YBM and PDSW models (Table 1). It was assumed that during flood tide the nitrate concentration at the mouth of the bay was equal to the concentration value in upwelled waters, $30 \mu\text{mol l}^{-1}$. During ebb tide, the August 2000 Yaquina Bay transect values (Fig. 3) were used to estimate concentrations in the plume. Plume concentration was a function of distance traveled by a water parcel moving towards the mouth. It was assumed that the nitrate level between the mouth of the estuary and at 1 km into the bay was $30 \mu\text{mol l}^{-1}$ near high slack water (the first 1 km of travel of a parcel), decreased linearly to $20 \mu\text{mol l}^{-1}$ at 3 km, and decreased further to the minimum level of about $5 \mu\text{mol l}^{-1}$ between 3 km and 12 km up-estuary, presumably due to biological uptake. Based on this model, the net flux of nitrate into the estuary on neap and spring tides was about $12,900 \text{ kg day}^{-1}$ (Table 1). This calculation can be compared to an earlier estimate of the maximum daily onshore nutrient transport during an 11-day upwelling event in which Atlas et al. (1977) estimated that $31 \text{ kg N day}^{-1} \text{ m}^{-1}$ were transported onshore along 1 m of coastline. This quantity of nitrate N would require interception of 832 m of coastline to provide $12,900 \text{ kg day}^{-1}$ into Yaquina Bay. In other words, $31 \text{ kg N day}^{-1} \text{ m}^{-1}$ is sufficient to supply the amount of nitrate predicted in the present work. A daily average influx taken over the upwelling season could be a factor of four or more times lower because upwelling events occur during approximately one quarter of the upwelling season. Atlas et al. (1977) also concluded that semi-diurnal tidal motion was important in onshore–offshore nutrient transport.

Modeling results and data interpretation support the hypothesis that, during ebb tide, the Yaquina estuary plume frequently influenced the chemical concentrations and physical parameters measured at the Yaquina Bay buoy and that water property changes could be estimated from model dilution predictions. The YBM current model supports the hypothesis that during periods of summer upwelling, the coastal ocean is a source of nitrate for the estuary. Although based on the steady-state assumption, the model shows that the estuarine plume can reach the buoy still possessing properties that can explain the nitrate depressions and offshore velocities.

In summary, a nitrate time series indicated that along shore nitrate concentrations near Yaquina Bay remained relatively high due to coastal upwelling throughout the month of August, even persisting during

short periods of downwelling. Both tidal cycle variability and longer variability due to a complex combination of wind forcing and biological utilization of nutrients were observed. Nitrate values at the OSU Dock were 30% lower than those of the ocean, indicating that nutrient uptake was significant within a short distance from the bay mouth. The nitrate-depleted estuarine water mass was exported from the estuary on the ebb tide and was carried past the moored sensors towards the open ocean. Our model postulates that tidally induced flow into the estuary imports higher-nitrate water and plume flow out of the estuary exports low-nitrate water such that the ocean is a net source of nitrate to the Yaquina estuary at this time.

Acknowledgments

We thank Capt. R. Barrel of the R/V Elakha for logistic support, W. Parker, W. Floering and R. Miller for design, deployment and recovery of the mooring, N. Kachel for supplying corrected wind data and processing some of the mooring data, S. Salo for processing satellite data, and W. Peterson, R. Burke, C. West and two anonymous reviewers for reviews of the manuscript. This work was funded by the Joint Institute for the Study of the Atmosphere and Ocean (JISAO) under NOAA Cooperative Agreement No. NA67RJ0155, and by EPA Interagency Agreement DW138956-01. This is JISAO's Coastal Ocean Program Contribution No. 900 and PMEL Contribution No. 2449. This document was subjected to EPA's peer and administrative review, and it was approved for publication. Mention of trade names or commercial products in this paper does not constitute endorsement or recommendation for use.

References

- Aminot, A., K erouel, R., 1998. Pasteurization as an alternative method for preservation of nitrate and nitrite in seawater samples. *Marine Chemistry* 61, 203–208.
- Atlas, E.L., Gordon, L.I., Thomlinson, R.D., 1977. Chemical characteristics of Pacific Northwestern coastal waters – nutrients, salinities, seasonal fluctuations. In: Krauss, R.W. (Ed.), *The Marine Plant Biomass of the Pacific Northwest Coast*. Oregon State University Press, Corvallis, pp. 57–79.
- Barth, J.A., Pierce, S.D., Smith, R.L., 2000. A separating coastal upwelling jet at Cape Blanco, Oregon and its connection to the California Current System. *Deep-Sea Research II* 47, 783–810.
- Chapman, J.W., Frick, W.E., Clinton, P.J., 1997. Critical tide effects and intertidal zonation revisited. *Proceedings of the 77th Annual Meeting, Western Society of Naturalists, La Paz, Mexico, Jan 8–11, 1997*.
- Compton, J.E., Church, M.R., Larned, S.T., Hogsett, W.E., 2003. Nitrogen export from forested watersheds in the Oregon coast range: the role of N_2 -fixing red alder. *Ecosystems* 6, 773–785.
- Davis, L.R., 1999. *Fundamentals of Environmental Discharge Modeling*. CRC, 165 pp.

- Dickey, T., Frye, D., Jannasch, H., Boyle, E., Manov, D., Sigurdson, D., McNeil, J., Stramska, M., Michaels, A., Nelson, N., Siegel, D., Chang, G., Wu, J., Knap, A., 1998. Initial results from the Bermuda Testbed Mooring program. *Deep-Sea Research I* 45, 771–794.
- Frick, W.E., Roberts, P.J.W., Davis, L.R., Keyes, J., Baumgartner, D.J., George, K.P., 2003. Dilution Models for Effluent Discharges, fourth ed. (Visual Plumes). EPA/600/R-03/025, Athens, GA <http://www.epa.gov/ceampubl/swater/vplume/index.htm>.
- Frick, W.E., Sigleo, A.C., Specht, D.T., 2004. Estimating nitrogen and tidal exchange in a North Pacific estuary with EPA's Visual Plumes PDSW model. Proceedings of the Third International Conference on Marine Waste Water Discharge, Catania, Italy Sept 27–Oct 2, 2004. P-S18, pp. 1–13.
- Gordon, L.I., Jennings Jr., J.C., Ross, A.A., Krest, J.M., 1993. A suggested protocol for continuous flow automated analysis of seawater nutrients (phosphate, nitrate, nitrite and silicic acid) in the WOCE Hydrographic program and the Joint Global Ocean Fluxes Study, WOCE Operations Manual, vol. 3: The Observational Programme, Section 3.2: WOCE Hydrographic Programme, Part 3.1.3: WHP Operations and Methods. WHP Office Report WHPO 91-1; WOCE Report No. 68/91. November, 1994, Revision 1, Woods Hole, MA, USA, 52 pp.
- Hickey, B.M., Banas, N.S., 2003. Oceanography of the U.S. Pacific Northwest coastal ocean and estuaries with application to coastal ecology. *Estuaries* 26, 1010–1031.
- Hydes, D.J., Wright, P.N., Rawlinson, M.B., 2000. Use of a wet chemical analyzer for the in situ monitoring of nitrate. In: Varney, M.S. (Ed.), *Chemical Sensors in Oceanography*. Gordon and Breach Publishing Group, pp. 95–105.
- Karl, D.M., Lukas, R., 1996. The Hawaii Ocean Time-series (HOT) program: background, rationale and field implementation. *Deep-Sea Research II* 43, 129–156.
- Kentula, M.E., DeWitt, T.H., 2003. Abundance of seagrass (*Zostera marina* L.) and macroalgae in relation to the salinity–temperature gradient in Yaquina Bay, Oregon, USA. *Estuaries* 26, 1130–1141.
- Larned, S.T., 2003. Effects of the invasive, nonindigenous seagrass *Zostera japonica* on nutrient fluxes between the water column and benthos in a NE Pacific estuary. *Marine Ecology Progress Series* 254, 69–80.
- Mantovanelli, A., Marone, E., da Silva, E.T., Lautert, L.F., Klingenfuss, M.S., Prata Jr., V.P., Noernberg, M.A., Knoppers, B.A., Angulo, R.J., 2004. Combined tidal velocity and duration asymmetries as a determinant of water transport and residual flow in Paranaguá Bay estuary. *Estuarine, Coastal and Shelf Science* 59, 523–537.
- National Oceanic and Atmospheric Administration (NOAA), 1984. NOAA's National Ocean Service, Coast Survey Nautical Chart 18581, Yaquina Bay and River. U.S. Department of Commerce, Washington DC.
- Sigleo, A.C., Frick, W.E., 2003. Seasonal variations in nutrient concentrations and river flow in a northwestern USA watershed. In: Renard, K.G., et al. (Eds.), *First Interagency Conference on Research in the Watersheds*. Benson, AZ, October 28–30. U.S. Department of Agriculture, pp. 370–375.
- Small, L.F., Menzies, D.W., 1981. Patterns of primary productivity and biomass in a coastal upwelling region. *Deep-Sea Research* 28, 123–149.
- Steinberg, D.K., Carlson, C.A., Bates, N.R., Johnson, R.J., Michaels, A.F., Knap, A.H., 2001. Overview of the US JGOFS Bermuda Atlantic Time-series Study (BATS): a decade-scale look at ocean biology and biogeochemistry. *Deep-Sea Research II* 48, 1405–1447.
- Strub, J.T., James, C., 2000. Altimeter-derived variability of surface velocities in the California Current System: 2. Seasonal circulation and eddy statistics. *Deep-Sea Research II* 47, 831–870.
- Takesue, R.K., van Geen, A., 2002. Nearshore circulation during upwelling inferred from the distribution of dissolved cadmium off the Oregon coast. *Limnology and Oceanography* 47, 176–185.
- van Geen, A., Husby, D.M., 1996. Cadmium in the California Current System: tracer of past and present upwelling. *Journal of Geophysical Research* 101, 3489–3507.
- van Geen, A., Takesue, R.K., Goddard, J., Takahashi, T., Barth, J.A., Smith, R.L., 2000. Carbon and nutrient dynamics during coastal upwelling off Cape Blanco, Oregon. *Deep-Sea Research II* 47, 975–1002.
- Wallner, E.P., 1995. *Tides*, 32 Barney Hill Rd, Wayland, MA 01778 (<http://epwallnr@world.std.com>).
- Weston, K., Jickells, T.D., Fernand, L., Parker, E.R., 2004. Nitrogen cycling in the southern North Sea: consequences for total nitrogen transport. *Estuarine, Coastal and Shelf Science* 59, 559–573.